Impact of structural irregularities on high-bite-rate pulse compression techniques in photonics crystal fibre

Bertrand Kibler, Christophe Finot

Impact of structural irregularities

on high bit-rate pulse compression techniques in photonic crystal fibre

B. Kibler and C. Finot

Authors' affiliations:

B. Kibler, C. Finot

Institut Carnot de Bourgogne, UMR 5209 CNRS-Université de Bourgogne, 21078 DIJON, FRANCE.

Contact Author: B. Kibler

Contact Address: Institut Carnot de Bourgogne, CNRS UMR 5209

9 Avenue Alain Savary, BP 47 870

21078 Dijon

FRANCE

Fax: +33 (0)3 80 39 59 71

Phone: +33 (0)3 80 39 59 32

Email: Bertrand.Kibler@u-bourgogne.fr

Abstract

The impact of structural irregularities on high bit-rate pulse compression techniques is evaluated in photonic crystal fibre. Specifically, we report more robust pulse compression to longitudinal fluctuations in the normal dispersion regime. We identify the physical limits of these pulse compression techniques in the presence of dispersion fluctuations and we confirm that state-of-the-art fabrication tolerances are sufficient for future experimental applications.

The advent of optical microstructured fibres was one of the most revolutionary progresses over the past decade in the field of nonlinear waveguide optics [1]. Indeed, photonic crystal fibres (PCF) offer a significant degree of freedom for the control of chromatic dispersion, such as exhibiting two zero dispersion wavelengths. Moreover, solid-core PCFs have also enabled the significant nonlinearity required for supercontinuum generation [2]. Thanks to the growing control of the manufacturing processes [1], the use of such microstructures in the area of telecom applications now becomes conceivable. If a low normal or anomalous dispersion is needed at these infrared wavelengths, it is typically convenient to work in the vicinity of the second zero dispersion wavelength (IR-ZDW) of such holey fibres. But in this case, the dispersion properties become increasingly dependent on the geometrical fluctuations of the microstructure. In this letter, we determine what impact these changes may have on two specific high bit-rate nonlinear applications at 40 GHz, namely pulse compression techniques by multiple four-wave mixing (MFWM) in the anomalous dispersion regime or by conversion into a parabolic pulses in the normal dispersion regime with subsequent linear compression [3]. We confirm that state-of-the-art fabrication tolerances are compatible with future experimental applications.

To examine the consequences of the microstructure longitudinal fluctuations, we consider the typical highly nonlinear PCF structure shown in Fig. 1(a) with a hexagonal photonic crystal cladding surrounding a central solid core defect. We assume a hole diameter d = 1.1 µm and pitch Λ = 1.2 µm corresponding to a IR-ZDW at 1564.4 nm. Standard beam propagation method simulations were used to calculate the variation in dispersion and effective area with frequency [4]. From a recent review on PCF [1], it is now realistic to manufacture the microstructure in air-glass PCF to accuracies of 10 nm on the scale of 1 µm. However, such fluctuations of structure parameters such as core diameter, hole diameter or pitch, are sufficient to induce significant variations of dispersion, nonlinearity and birefringence characteristics, which are highly detrimental to nonlinear processes [5-7]. In the following analysis, we focus on large dispersion variations induced by

longitudinal fluctuations of the pitch Λ while the diameter-to-pitch ratio d / Λ remains constant. Indeed, Fig. 1(b) outlines the significant dependence of the dispersion on pitch variations about 1-2%. Note that pitch fluctuations of ±1% lead to variations as high as ±16 nm in the position of the IR-ZDW, equivalent to a ±110% fluctuation of the GVD value at 1550 nm. Such extreme dependences have already been reported experimentally [8]. The nonlinear coefficient γ is found to be less sensitive ($\delta\gamma < 1\%$) and its variations will be neglected ($\gamma \approx 63$ W^{-1} km^{-1} for the considered range of wavelengths). Therefore, we investigate the impact of such dispersion fluctuations on two pulse compression applications. In both cases, an initial sinusoidal signal obtained from the beating of two continuous laser diodes is compressed in order to generate picosecond pulse trains at 40 GHz (see Fig. 2).

The first method (Fig. 2(a)) is based on a MFWM process taking place in the anomalous dispersion regime and simultaneoulsy leading to a strong spectral broadening and a temporal compression of the sinusoidal signal [9]. Consequently, we consider the central wavelength of the laser diodes fixed to 1550 nm where the corresponding GVD is D = 9.92 ps/km·nm. Generalized nonlinear Schrödinger equation (GNLSE) simulations including the global dispersion characteristics [2] were used to determine the corresponding output pulses. From [9], the optimum input average power and fibre length, for a maximum compression and minimum chirp, were respectively found to P_{opt} = 5.1 mW and L_{opt} = 3.5 km. Our numerical simulations confirm these optimal values in the absence of dispersion fluctuations and Fig. 2(a) shows that the initial sinusoidal train is efficiently converted into a 40-GHz nearly Gaussian pulses train with a FWHM temporal width of 4.2 ps. In order to characterize the output pulse shape, we computed the misfit parameter M_{opt} between the pulse intensity profile and a Gaussian fit of the same energy [10]. To approach a realistic description of random fluctuations of the pitch parameter and subsequent dispersion fluctuations, we consider the randomly varying part of the pitch as a real, Gaussian, stationary stochastic process with zero mean [5]. For each simulated step of propagation, the corresponding GVD curve is then determined from the random

value of the pitch. Varying the standard deviation σ and the correlation length L_C (fluctuation period) of the distribution, we have drawn maps in Fig. 3(a) and (b), illustrating variations of the output pulse temporal width T_{OUT} (FWHM) in percentage and the normalized misfit parameter (M/M_{opt}). Here, the largest standard deviation of the pitch taken into account is 0.55% which corresponds to a maximal variation of the pitch around 2% (~4σ) and the largest correlation length is the PCF length. Each point of these maps has been calculated from an ensemble of 50 simulations. From Fig. 3(a), we globally note that a standard deviation of Λ below 0.2% leads to an acceptable fluctuation of T_{OUT} inferior to 10%. In the case of higher standard deviations, the group-velocity dispersion may become normal and lead to local temporal broadening of the pulses. This then explains large variations up to 100% of T_{OUT} (not shown by the color scale used) and over 40×M_{opt} in the normalized misfit parameter (see Fig. 3(b)). For long-scale fluctuations and high standard deviations, these results show how this nonlinear pulse compression technique is extremely sensitive to local GVD variation (in particular its sign) during propagation. However, we generally observe from Fig. 3(a-b) that when $L_C \rightarrow 0$, the effect of the fluctuations disappears whatever the standard deviation. Short-scale fluctuations of the pitch inferior to $L_{PCF}/40$ (corresponding to $\gamma P_0 L_C << 1$) have poor impact, in agreement with previous results demonstrated in the context of parametric amplification [7].

The second method (Fig. 2(b)) of 40-GHz pulse train generation relies on the progressive reshaping of the initial sinusoidal beat-signal into a train of linearly chirped quasi-parabolic pulses in the normal dispersion regime [10]. After linear compression of the parabolic pulses into a standard optical fibre with opposite dispersion (SMF-28), a train of well-separated picosecond pulses is achieved [3]. Here, we consider the central wavelength of the laser diodes fixed to 1580 nm, where the GVD is D = -10.55 ps/km·nm. The optimum input average power and fibre length [10], for a quasi-linear chirp across the pulses and minimum overlapping between consecutive pulses, were respectively found to P_{opt} = 7 mW and L_{opt} = 1.5 km. The anomalous dispersive compression fibre is a SMF with the following fixed parameters: D_{SMF} = 17.8 ps/km·nm, dispersion slope S_{SMF} = 0.057

ps/km·nm^2, nonlinear coefficient γ_{SMF} = 1.2 W^{-1} km^{-1} and optimum length L_{SMF} = 1.25 km. The ouput pulses have a nearly Gaussian intensity profile with a 7.6 ps (FWHM) temporal width and the new optimal computed misfit parameter is M_{opt}. Following the previous modeling of random fluctuations, Fig. 3(c) and (d) show variations of T_{OUT} in percentage and the normalized misfit parameter (M/M_{opt}) obtained for this pulse compression technique. From Fig. 3(c), we observe that a standard deviation of Λ inferior to 0.2% only corresponds to a fluctuation of T_{OUT} below 5%. For higher standard deviation, the group-velocity dispersion can become anomalous and now leads to local temporal compression of the pulses in PCF, however variations of T_{OUT} remain inferior to 15% and those of the normalized misfit parameter do not exceed 20×M_{opt} (see Fig. 3(d)). Indeed, the first propagation stage in PCF broadens the pulses and decreases the peak power before linear compression. The impact of local GVD fluctuations is then weaker than in the nonlinear compression technique. This explains the “smoothing” of fluctuations maps. As the previous technique, we also observe from Fig. 3(c-d) that when $L_C \rightarrow 0$, the effect of the fluctuations vanishes.

In conclusion, these results demonstrate that longitudinal fluctuations of microstructure parameters in PCF are not detrimental for high bit-rate pulse compression techniques thanks to best current fabrication tolerances around 1% (σ~0.25%) on the scale of 1 µm. Moreover, we have identified more robustness in the normal dispersion regime. We expect that these required tolerances encourage the use of kilometer-long PCF for future high bit-rate nonlinear experimental applications.

Acknowledgements: This research was supported by the Agence Nationale de la Recherche (SUPERCODE project, ANR-06-BLAN-0401).

References

1. P. St. J. Russell, " Photonic-Crystal Fibers," Journal of Lightwave Technology **24**, 4729-4749 (2006).
2. J. M. Dudley, G. Genty, S. Coen, “Supercontinuum generation in photonic crystal fiber,” Reviews of Modern Physics **78**, 1135-1184 (2006).
3. S. Pitois, C. Finot, J. Fatome, B. Sinardet, G. Millot, “Generation of 20-GHz picosecond pulse trains in the normal and anomalous dispersion regimes of optical fibers,” Optics Communications **260**, 301-306 (2006).
4. BeamPROP 5.1 (RSoft. Design Group, Inc., NY 2003).
5. M. Karlsson, " Four-wave mixing in fibers with randomly varying zero-dispersion wavelength," Journal of the Optical Society of America B **15**, 2269-2275 (1998).
6. B. Kibler, C. Billet, J. M. Dudley, R. S. Windeler, G. Millot, “Effects of structural irregularities on modulational instability phase matching in photonic crystal fibers,” Optics Letters **29**, 1903-1905 (2004).
7. M. Farahmand, M. de Sterke, “Parametric amplification in presence of dispersion fluctuations,” Optics Express **12**, 136-142 (2004).
8. N. Y. Joly, F. G. Omenetto, A. Efimov, A. J. Taylor, J. C. Knight, P. S. J. Russell, “Competition between spectral splitting and Raman frequency shift in negative-dispersion slope photonic crystal fiber,” Optics Communications **248**, 281-285 (2005).
9. J. Fatome, S. Pitois, G. Millot, “20-GHz-to-1-THz repetition rate pulse sources based on multiple four-wave mixing in optical fibers,” IEEE Journal of Quantum Electronics **42**, 1038-1046 (2006).
10. C. Finot, L. Provost, P. Petropoulos, D. J. Richardson, “Parabolic pulse generation through passive nonlinear pulse reshaping in a normally dispersive two segment

fiber device," Optics Express **15**, 852-864 (2007).

Figure Captions:

Fig. 1 (a) PCF dispersion curve obtained for the following microstructure parameters : hole diameter d = 1.1 µm and pitch Λ = 1.2 µm. (b) Dispersion variations induced by fluctuations ($\delta \Lambda$) of the pitch in the vicinity of the IR-ZDW.

Fig. 2 Setup diagram with the input sinusoidal signal at 40 GHz, (a) for MFWM compression and (b) for parabolic pulses generation and linear compression.

Fig. 3 Numerical results showing variations of (a,c) the output temporal width T_{OUT} (in percentage) and (b,d) the normalized misfit parameter (M/M_{opt}) as functions of both the standard deviation σ and the correlation length L_C of the pitch fluctuations, for compression techniques in anomalous (a,b) and normal (c,d) dispersion regimes.

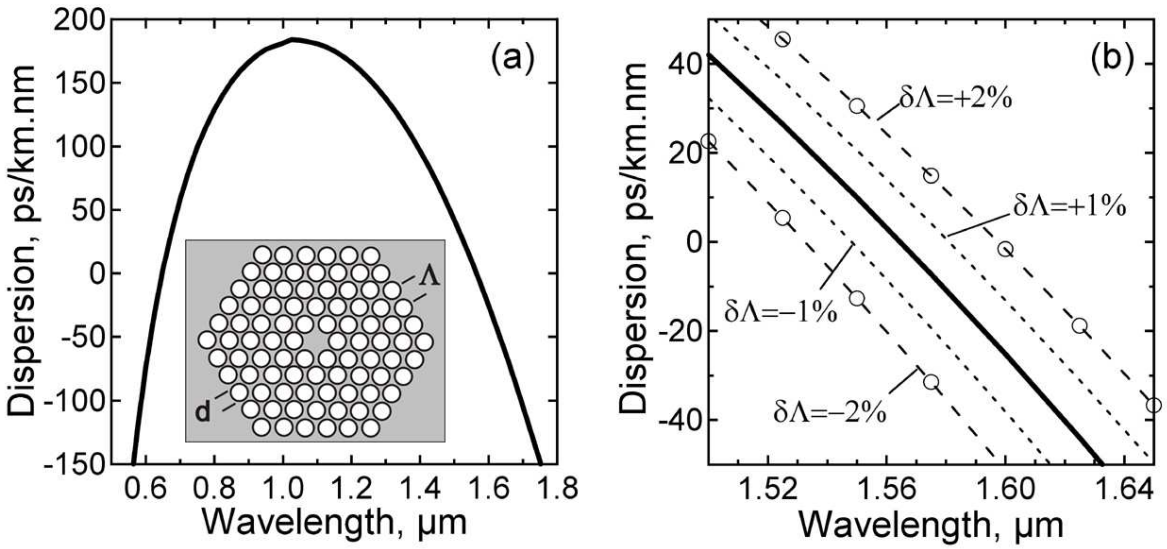
(a)
Dispersion, ps/km.nm
Wavelength, μm
Λ
d
(b)
δΛ=+2%
δΛ=+1%
δΛ=−1%
δΛ=−2%
Dispersion, ps/km.nm
Wavelength, μm

FIGURE 1

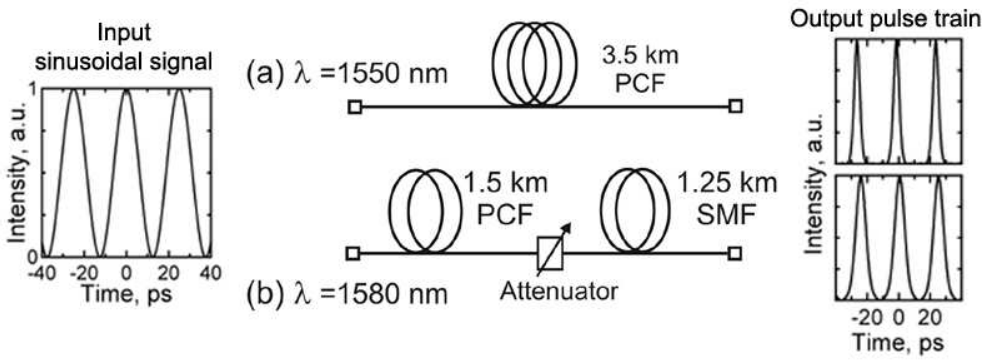
Input
sinusoidal signal
Intensity, a.u.
1
0
-40 -20 0 20 40
Time, ps
(a) λ =1550 nm
3.5 km
PCF
1.5 km
PCF
1.25 km
SMF
Attenuator
(b) λ =1580 nm
Output pulse train
Intensity, a.u.
-20 0 20
Time, ps

FIGURE 2

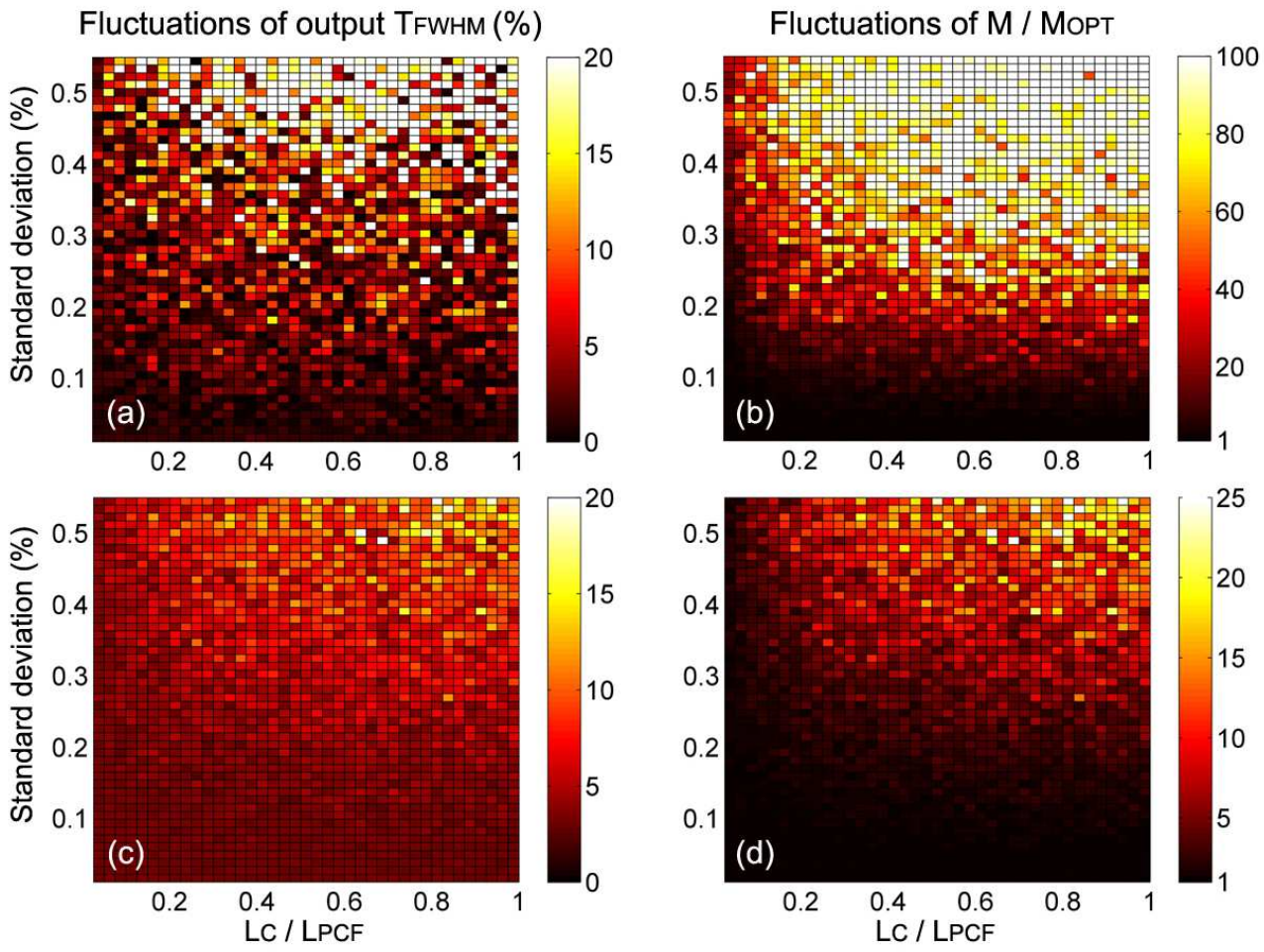
Fluctuations of output TFWHM (%)
Fluctuations of M / MOPT
Standard deviation (%)
Standard deviation (%)
(a)
(b)
(c)
(d)
0.1
0.2
0.3
0.4
0.5
0.2
0.4
0.6
0.8
1
0
5
10
15
20
1
20
40
60
80
100
1
5
10
15
20
25
LC / LPCF
LC / LPCF

FIGURE 3